Lab 4: Lift & Drag of a Finite Wing

Gregory Golonka, Connor Hack, and Timothy Welch

April 2024

Abstract

This lab explores the differences between the analytical and experimental solutions for finite wing analyses. During this lab a force balance was used to measure the resultant forces acting on six different finite wing geometries: testing the differences in aspect ratio; taper ratio; an elliptic distribution; and the addition of a winglet. The experimental data was then compared to results using Prandtl's lifting-line theory. Some notable results from the lab are that the experimental lift curve slopes were all less than the value of $m_0 = 2\pi$ per radian, that the addition of wing taper reduces total and induced drag, and that the addition of the winglet increased the coefficient of drag by 0.022, despite decreasing the induced drag. Furthermore, the winglet increased the lift curve slope by 0.016 compared to the base wing model.

1 Introduction

The goal of this lab was to use a force balance to measure the lift and drag generated by wings of various aspect and taper ratios. The experiments conducted also measured the resultant forces with a winglet. This experimental data was then compared to predictions from thin-airfoil and lifting line theory. By comparing the experimental and analytical data, the experiment shows the accuracy of Prandtl's lifting line theory, and any limitations in its usage moving forward.

1.1 Lifting Line Theory

The theoretical portion of this lab focuses on Prandtl's lifting line theory. Lifting-line theory allows for an analysis of finite wings. The underlying assumption treats the wing as a bound vortex along its center of pressure. This assumption falls short because actual finite wings have non-constant vortex strength. As such, the wing is modeled as a collection of superimposed bound vortices, of varying strength, along the span of the wing. For the purpose of this lab, the fundamental equation of Prandtl's lifting line theory was approximated using a Fourier sine series as defined in the Foundations of Aerodynamics by Kuethe and Chow. [1]:

$$\alpha_0(\theta) = \frac{m_0 c|_s}{m_0 c|_\theta} \sum_{n=1}^{\infty} a_n \sin n\theta + \frac{m_0 c|_s}{4b} \sum_{n=1}^{\infty} n a_n \frac{\sin n\theta}{\sin \theta} \tag{1}$$

Where m_0 is the lift curve slope, $c|_s$ is the chord length about the symmetric axis and $c|_\theta$ is the chord length at a point θ along the span b. The theory was then used in this experiment to calculate theoretical values of the coefficients of lift and drag.

2 Experimental Setup

2.1 Define Ambient Conditions

The ambient conditions of the laboratory were measured for the period in which the experiment was conducted. The ambient pressure and temperature were obtained from a Fisher Scientific Traceable digital barometer within the testing room. This data was taken at both the beginning and end of the lab duration. The temperature and pressure data can be used to calculate the air density with the Ideal Gas Law given in the equation

$$\rho = \frac{P}{RT} \tag{2}$$

where ρ is the density, P is the ambient pressure, R is the specific gas constant of air taken to be 287 $\frac{\text{J}}{\text{kg}\cdot\text{K}}$, and T is the temperature. The values of P, T, and ρ taken and calculated for both times, as well as their averages, are tabulated in Table 1.

Table 1: Ambient conditions of the lab before and after the experiments.

Time	Temperature, T (K)	Pressure, P (Pa)	Density, ρ ($\frac{\text{kg}}{\text{m}^3}$)
5:16pm	295.35	9.80E+04	1.16
7:50pm	295.45	9.83E+04	1.16
Average	295.4 ± 0.6	9.82E+04 $\pm$ 400	1.16 ± 0.01

The uncertainties in these measurements are important to the later analysis. The uncertainties in the average pressures, temperature, and density were calculated by propagating component uncertainties in quadrature. The component uncertainties from the above-stated measurement device are listed in Table 2.

Table 2: Uncertainty of pressure and temperature measurements.

Source	Pressure, ϵ_P (Pa)	Temperature, ϵ_T (K)
Reading	100	0.1
Systematic	400	0.4
Drift	100	0.4

The uncertainty in density was calculated from the quadrature addition of these uncertainties via the equation

$$\epsilon_\rho = \sqrt{\left(\frac{\epsilon_P}{RT}\right)^2 + \left(\frac{-\epsilon_T P}{T^2}\right)^2} \tag{3}$$

where ϵ_ρ is the uncertainty in density, ϵ_P is the uncertainty in pressure, and ϵ_T is the uncertainty in temperature. This was the same process used in Lab 1: Transducer Calibration & Pitot Wake Profiles.

2.2 Testing Apparatus

A brief discussion of the wind tunnel used in this lab is also relevant. The lab was conducted using a turbine-type wind tunnel found in the Hessert Laboratories on the University of Notre Dame campus. The tunnel fluctuates the freestream velocity as a percentage of the maximum motor speed. The flow velocity was held constant throughout the duration of the Airfoil Pressure Distribution Lab. The schematic for the wind tunnel can be found in Figure 1. The schematic for the wind tunnel comes from the Lab 2 Circulation around a 2-D Airfoil Measured with a Five-Hole Probe lab handout [2].

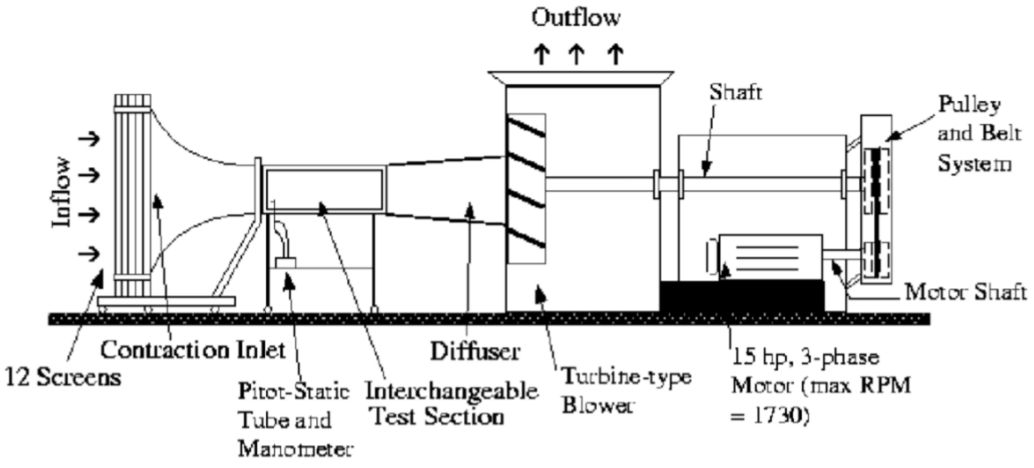

Figure 1: Informational graphic describing the different parts of a turbine-type wind turbine.

3 Experimental Procedure

The following procedure comes from the lab handout [3].

3.1 Preparing Experiment

Before the experiment could be conducted, a few steps had to be taken to ensure it ran smoothly. First, the pitot probe was checked to be oriented parallel to the direction of the flow. This ensures that the pressure data collected was accurate to the testing conditions. After the pitot probe was aligned, the static line was connected to the top port, and the stagnation line was connected to the bottom port. Next, the Analog In connections were checked: AI0 $\rightarrow$ pressure; AI1 $\rightarrow$ lift; AI2 $\rightarrow$ drag; AI3 $\rightarrow M_{\frac{1}{2}\bar{c}}$. This step was done by the TA before the lab was conducted, but the connections were still checked to maintain good

lab practice. Finally, the motor controller was set to the second input and the DAQ Utility was plugged into power.

3.2 Test Articles

This lab looked at the lift and drag generation of six different wing profiles. These test articles all shared the same NACA 0015 profile but varied in their aspect and taper ratios. Moreover, they are unswept and have zero dihedral. Table 3 summarizes the geometries of the six half wings tested throughout the lab. Using these wing geometries, the lift, drag and moment about the half chord were measured from $-20°$ to $20°$ in $1°$ increments.

Table 3: Wing Models

Wing #	$b/2$ (in)	$\bar{c}$ (in)	$S/2$ (in^2)	AR	c_t/c_r	Changing	Note
1	10	5	50	4	1	-	
2	7.91	6.32	50	2.5	1	Smaller AR	
3	12.5	4	50	6.25	1	Larger AR	
4	10	5	50	4	3/7	Taper	
5	10	3.93	39.27	5.09	ellip.	Elliptic	
6	10	5	50	4	1	Winglet	Attach winglet on AR = 4 wing

3.3 Force Balance

This lab uses a force balance to measure the resultant forces generated by the various wing geometries. The force balance sat below the center of the test section and had a metal dowel protruding into the wind tunnel. This dowel, or sting, connected to the different wing testing articles and locked them in place with a set screw. The force balance uses a Kistler 9306A 6-component piezoelectric force-torque sensor to measure the three force components and torque about the three normal axes. The force sensor outputs the forces and moments as voltages, which were converted using the calibration constants found in Table 4.

Table 4: Calibration constants for Kistler LabAmp Type 5167A force balance.

Direction	Sensitivity
F_L	0.02 (V/N)
F_D	0.02 (V/N)
$M_{\frac{1}{2}\bar{c}}$	0.025 (V/Nm)

4 Results and Analysis

4.1 Voltage Conversion Calculations

For further visualizations and analysis, certain values from the lab are necessary. Using the voltage data measured in lab, the force of lift, the force of drag, and the moment about the half chord can be determined with the equation

$$(V_{measured} - V_{offset}) \cdot \frac{1}{Sensitivity} = Output \tag{4}$$

where $V_{measured}$ is the voltage read in from the DAQ Utility, V_{offset} is the measured voltage offset measured in 3.3 Force Balance, *Sensitivity* relates to the desired value sensitivity found in Table 4, and *Output* is the desired value. This equation is the foundation from which further analysis and visualization are built upon.

The uncertainty of the voltage output was calculated by propagating the uncertainty in quadrature. The uncertainty of the output can be defined as:

$$\epsilon_{Out} = \sqrt{\left(\frac{1}{S}\epsilon_{V_{Meas}}\right)^2 + \left(\frac{1}{S}\epsilon_{V_{Off}}\right)^2} \tag{5}$$

where S is the planform area, and $\epsilon_{V_{Meas}}$ and $\epsilon_{V_{Off}}$ are the uncertainties of the measured and offset voltages. The uncertainty values for the voltage come from the spec sheet attached to the Lab Handout [3].

4.2 Lift

As it is one of the most relevant aspects of flight, an understanding of how lift varies with the angle of attack of a given wing is vital. Lift is calculated in this experiment using the lift channel voltage outputs in Eq. 4. Furthermore, the uncertainty in the lift is determined by Eq. 5. Figure 2 depicts the lift generated by each wing and their accompanying uncertainties over the full range of angles of attack.

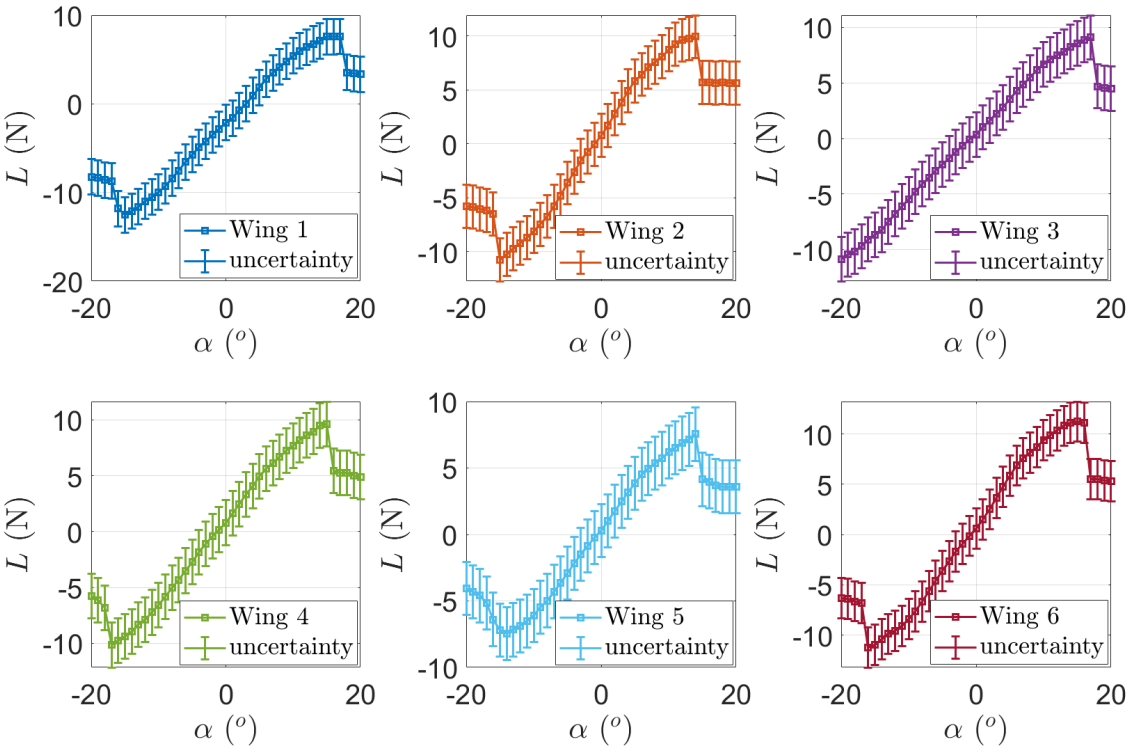

Figure 2: Lift vs angle of attack for each wing.

From Figure 2 one can observe the stall angles for each wing in the positive and negative angle of attack regimes. These values were determined by inspection and tabulated in Table 5.

Table 5: Various lift curve slopes for each of the wings tested in lab.

Wing #	**Positive Stall Angle (°)**	**Negative Stall Angle (°)**
1	17	-15
2	17	-20
3	14	-15
4	15	-17
5	14	-14
6	16	-16

The coefficient of lift is also useful for understanding the wing because it serves as a non-dimensionalized lift. As mentioned in Section 1.1, Prandtl's Lifting Line theory can be used to calculate the coefficient of lift for both an airfoil and wing. Specifically, the airfoil coefficient, c_L, is determined at every cross-sectional station of the wing, and the wing coefficient, C_L, is for the entire wing and therefore constant across the span. These theoretical,

non-dimensionalized lifts are highly valuable as they allow for comparison with any experimental data gathered. Figure 3 depicts a plot of both the wing and airfoil coefficients of lift across the span for several angles well within the stall angle range.

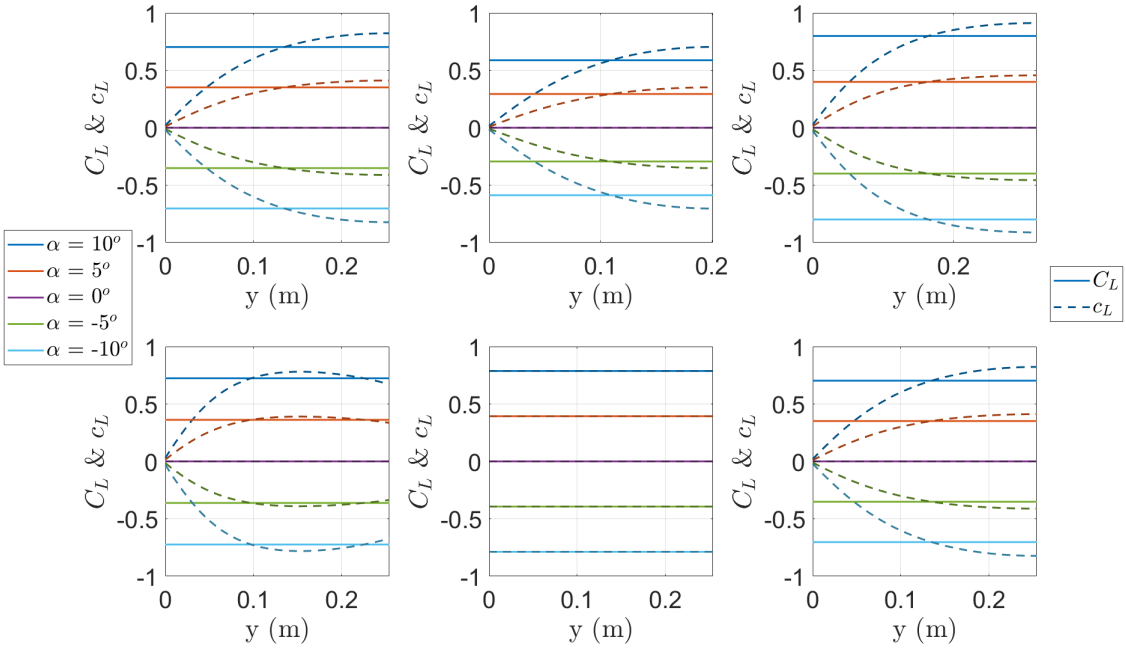

Figure 3: Coefficients of lift for wing and airfoil across half span of each wing.

Visualizing the experimental coefficient of lift as a function of the angle of attack for each wing is also beneficial for understanding finite wings and the effects of winglets. With the lift value determined for each wing, the coefficient of lift for each wing was determined with the equation

$$C_L = \frac{L}{q_\infty S} \tag{6}$$

where L is the lift, q_∞ is the dynamic pressure and S is the planform area of the wing. The dynamic pressure was determined by the difference in pressure measured during the experiment. The coefficient of lift as a function of angle of attack determined by Eq. 6 are plotted in Figure 4. The uncertainty of the lift coefficient was calculated similarly to the voltage output. By propagating any uncertainties in quadrature as defined:

$$\epsilon_{C_L} = \sqrt{\left(\epsilon_L \frac{1}{dPS}\right)^2} = \epsilon_L \frac{1}{dPS} \tag{7}$$

where ϵ_L is the uncertainty in lift, dP is the difference in pressures, and S is the planform area.

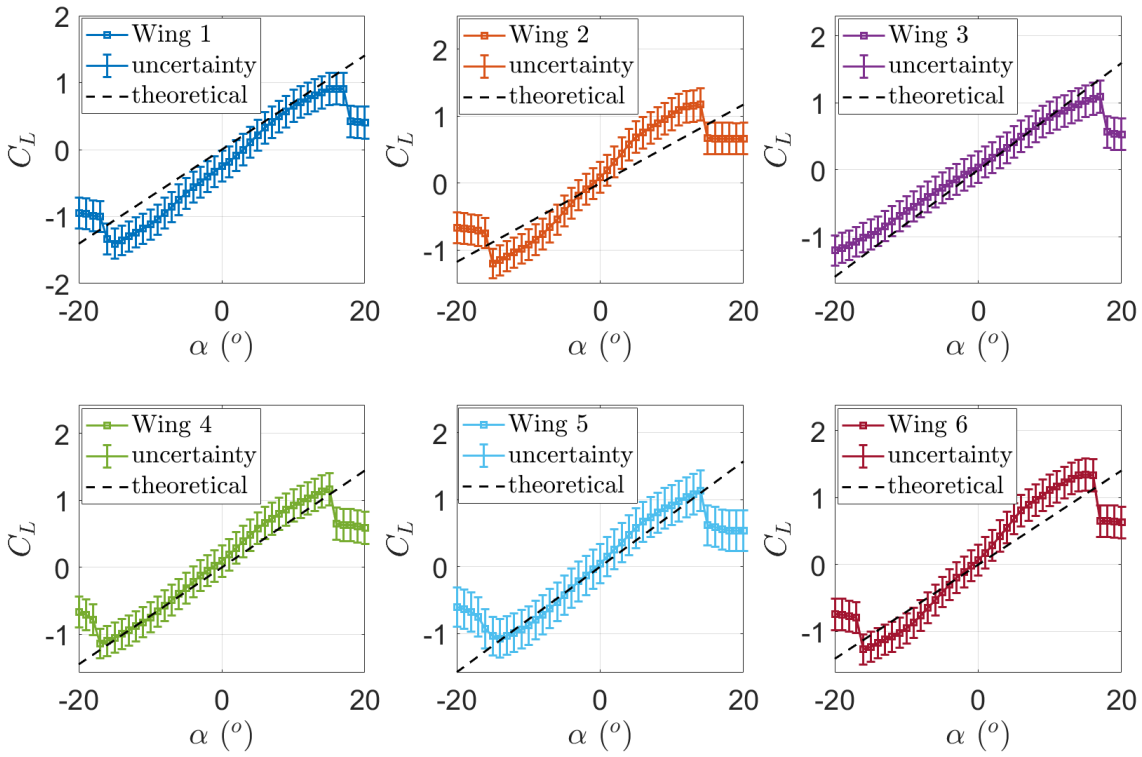

Figure 4: Coefficient of lift vs angle of attack for each wing.

It is also worth analyzing the lift curve slope for each of the wings as a function of angle of attack. Three lift curve slopes are relevant for this analysis: the lift curve slope of a 2D wing, the theoretical lift curve slope of a 3D wing, and the experimental lift curve slope determined through data analysis. The lift curve slope of a 2D wing is given by the equation

$$m_0 = \frac{\partial C_L}{\partial \alpha} = 2\pi \tag{8}$$

where m_0 is the lift curve slope and the value 2π is in radians. Moreover, the theoretical lift curve slope is given by Prandtl's lifting line equation

$$m_{theo} = \frac{A_1 \pi^2}{1+\lambda} \tag{9}$$

where A_1 is the first coefficient in the Fourier's series and λ is the taper ratio given as c_t/c_r, which is known from each wing. The experimentally determined lift curve slope for each wing was found using a line of best fit for the lift vs angle of attack data. Table 6 displays the lift curve slopes for each of the wing, including the lift curve slope if the wings were considered 2D, the theoretical slope via Prandtl's lifting line, and the actual lift curve slope determined from the experimental data. All the data presented is in the inverse of degrees.

Table 6: Various lift curve slopes for each of the wings tested in lab.

Wing #	m_0	m_{theo}	m	$\pm\epsilon_m$
1	0.110	0.0703	0.0870	0.0014
2	0.110	0.0587	0.0984	0.0015
3	0.110	0.0798	0.0695	0.0013
4	0.110	0.0723	0.0835	0.0020
5	0.110	0.0787	0.0908	0.0021
6	0.110	0.0703	0.102	0.002

To visualize the small differences between the lift slope for the different wing geometries, the differences between individual slopes were tabulated in Table 7. These differences were calculated both comparing each wing to wing 1 ($\Delta m_{\rightarrow 1}$) and comparing each wing to its own theoretical ($\Delta m_{\rightarrow theory}$) such that comparisons for the varying aspect ratio, taper ratio and the addition of the winglet could be made in section 5.1.

Table 7: Difference between lift slope for wing geometry and theoretical data.

Wing #	$\Delta m_{\rightarrow 1}$	$\epsilon_{\Delta m_{\rightarrow 1}}$	$\Delta m_{\rightarrow theory}$	$\epsilon_{\Delta m_{\rightarrow theory}}$
Wing 1	0	0	0.0167	0.0014
Wing 2	0.0114	0.0021	0.0397	0.0015
Wing 3	-0.0175	0.0019	-0.0103	0.0013
Wing 4	-0.00349	0.00252	0.0111	0.0020
Wing 5	0.00385	0.00256	0.0121	0.0021
Wing 6	0.0159	0.0023	0.0326	0.0018

4.3 Drag

An understanding of the drag generated by a wing and how that varies with the angle of attack is also vital. Similar to lift, drag is calculated with Eq. 4, and its uncertainty is calculated with Eq. 5. Figure 5 depicts the relationship between the drag of each wing along with their uncertainties and the angle of attack.

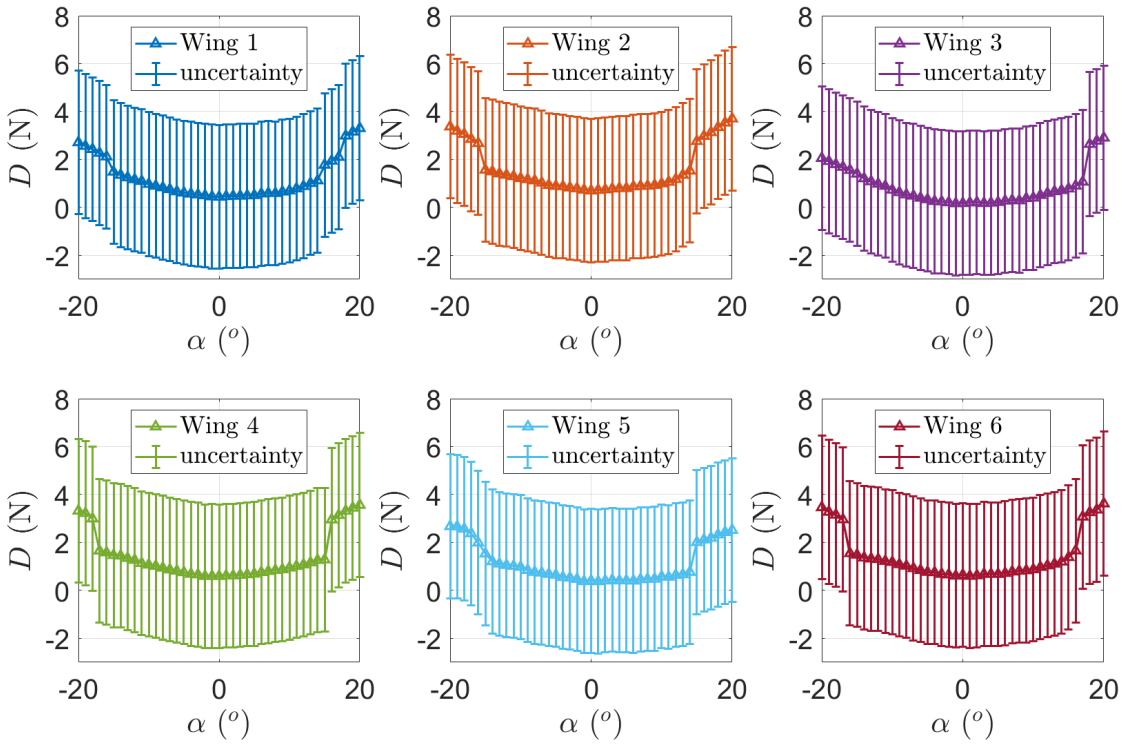

Figure 5: Drag vs angle of attack for each wing.

It is similarly of interest to analyze the coefficient of drag experienced by each wing. With the drag value experienced by the entire wing, the coefficient of drag was determined with the equation

$$C_D = \frac{D}{q_\infty S} \tag{10}$$

where C_D is the coefficient of total drag over the whole wing, and D is drag. From the determined coefficient of drag, the coefficient of drag as a function of the angle of attack is plotted in Figure 6.

The uncertainty of the drag coefficient was calculated the same as the lift coefficient. Using equation 10 the uncertainty of drag can be propagated through the data as defined:

$$\epsilon_{C_D} = \sqrt{\left(\epsilon_D \frac{1}{dPS}\right)^2} = \epsilon_D \frac{1}{dPS} \tag{11}$$

where ϵ_D is the uncertainty in drag.

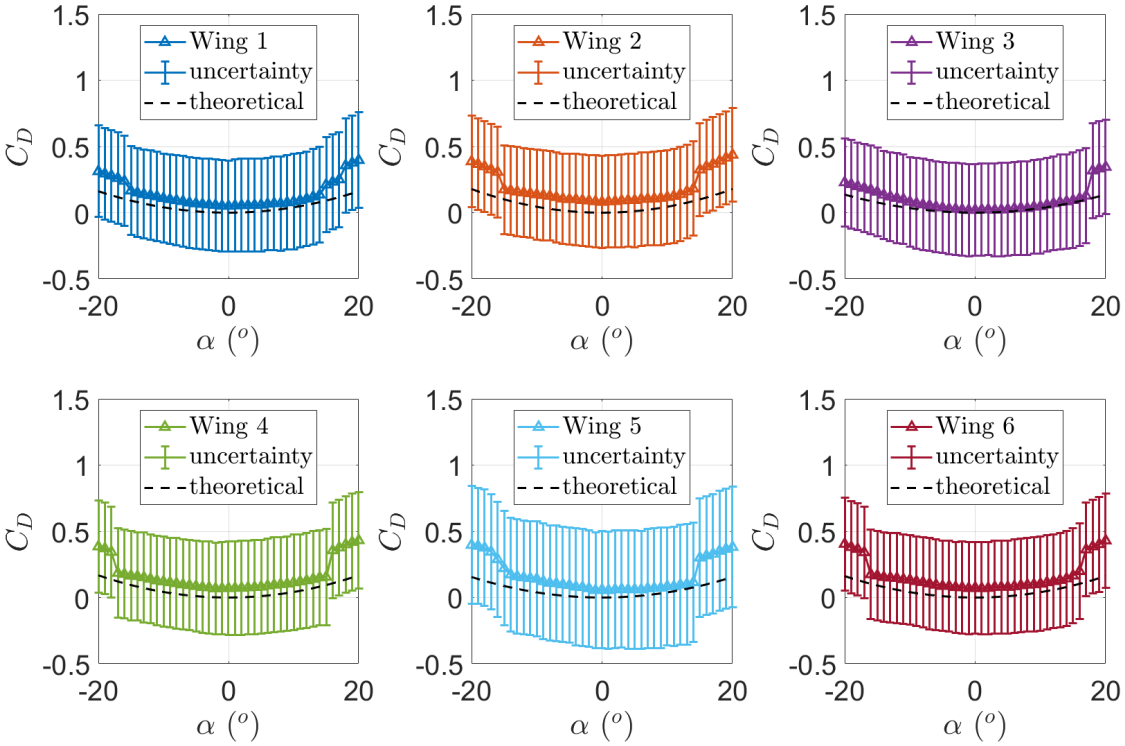

Figure 6: Coefficient of drag vs angle of attack.

To visualize the small differences between the drag coefficients for the different wing geometries, the differences were tabulated in Table 8. In a similar way to the lift slope calculations, these differences were calculated between wing 1 and the theoretical such that comparisons for the varying aspect ratio, taper ratio and the addition of the winglet could be made in section 5.2.

Table 8: Difference between drag coefficients for wing geometries and theoretical data.

Wing #	$\overline{\Delta C}_{D_{\to 1}}$	$\epsilon_{\overline{\Delta C}_{D_{\to 1}}}$	$\overline{\Delta C}_{D_{\to theory}}$	$\epsilon_{\overline{\Delta C}_{D_{\to theory}}}$
1	0	0	0.0861	0.0544
2	0.0423	0.0767	0.123	0.054
3	-0.0443	0.0768	0.0506	0.0542
4	0.0219	0.0771	0.106	0.055
5	0.0222	0.0879	0.111	0.069
6	0.0224	0.0769	0.109	0.054

4.4 Pitching Moment

In addition to the lift and drag, the moment about the quarter chord also bears discussion. The pitching moment, too, is calculated by Eq. 4 and its uncertainty by Eq. 5. However, the output is in units of $\mathrm{N}\cdot\mathrm{m}$ rather than N as it was for lift and drag. Additionally, Eq. 4 outputs the moment about the half-chord rather than the quarter-chord, which is the location of primary interest as it is the aerodynamic center of the wing. The quarter-chord moment is calculated from the half-chord moment using the equation

$$M_{\frac{1}{4}\overline{c}} = M_{\frac{1}{2}\overline{c}} - \frac{\overline{c}}{4}\left(L\cos\alpha - D\sin\alpha\right) \tag{12}$$

where $M_{\frac{1}{4}\overline{c}}$ is the pitching moment about the quarter-chord, $M_{\frac{1}{2}\overline{c}}$ is the pitching moment about the half-chord, and α is the angle of attack. The uncertainty of the moment about the quarter chord was found by propagating the uncertainty through equation 12. The uncertainty is defined as

$$\epsilon_{M_{c/4}} = \sqrt{\epsilon_{M_{c/2}}^2 + \left(\epsilon_L \frac{c}{4}\cos\alpha\right)^2 + \left(\epsilon_D \frac{c}{4}\sin\alpha\right)^2} \tag{13}$$

where $\epsilon_{M_{c/2}}$ is the uncertainty of the moment about the half-chord, and $\epsilon_{M_{c/4}}$ is the uncertainty of the moment about the quarter-chord. The quarter-chord moment and its uncertainty are plotted for each wing against the angle of attack in Figure 7.

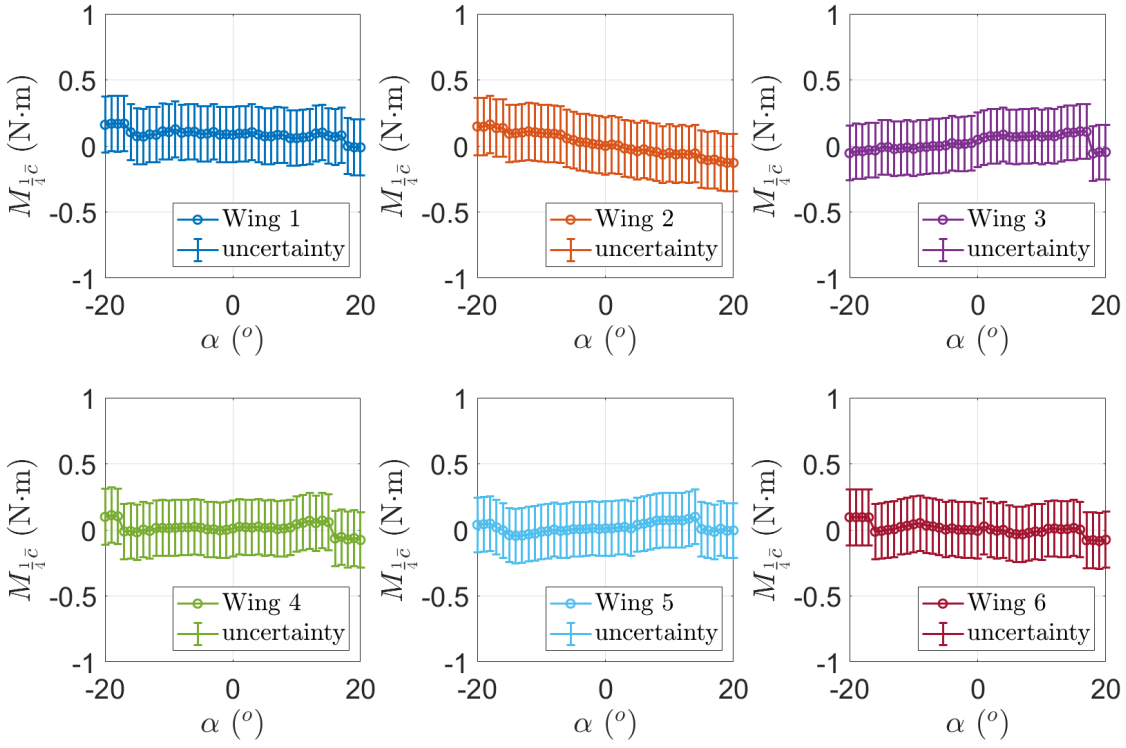

Figure 7: Quarter-chord pitching moment vs angle of attack for all wings.

The non-dimensionalized coefficient of the pitching moment about the quarter-chord, which makes comparison between the wings easiest, is also important to visualize. It is calculated with the equation

$$C_{M_{\frac{1}{4}\bar{c}}} = \frac{M_{\frac{1}{4}\bar{c}}}{q_\infty Sc} \tag{14}$$

where c is the chord length, and $C_{M_{\frac{1}{4}}}$ is the coefficient of the quarter chord moment. Its uncertainty is propagated via the equation

$$\epsilon_{C_{M_{\frac{1}{4}\bar{c}}}} = \sqrt{\left(\epsilon_L \frac{1}{dPS}\right)^2} = \epsilon_L \frac{1}{dPSc} \tag{15}$$

where $\epsilon_{C_{M_{\frac{1}{4}\bar{c}}}}$ is the uncertainty in the quarter-chord pitching moment coefficient. The coefficient of the quarter-chord pitching moment and its accompanying uncertainty are plotted in Figure 8 against the angle of attack for each wing.

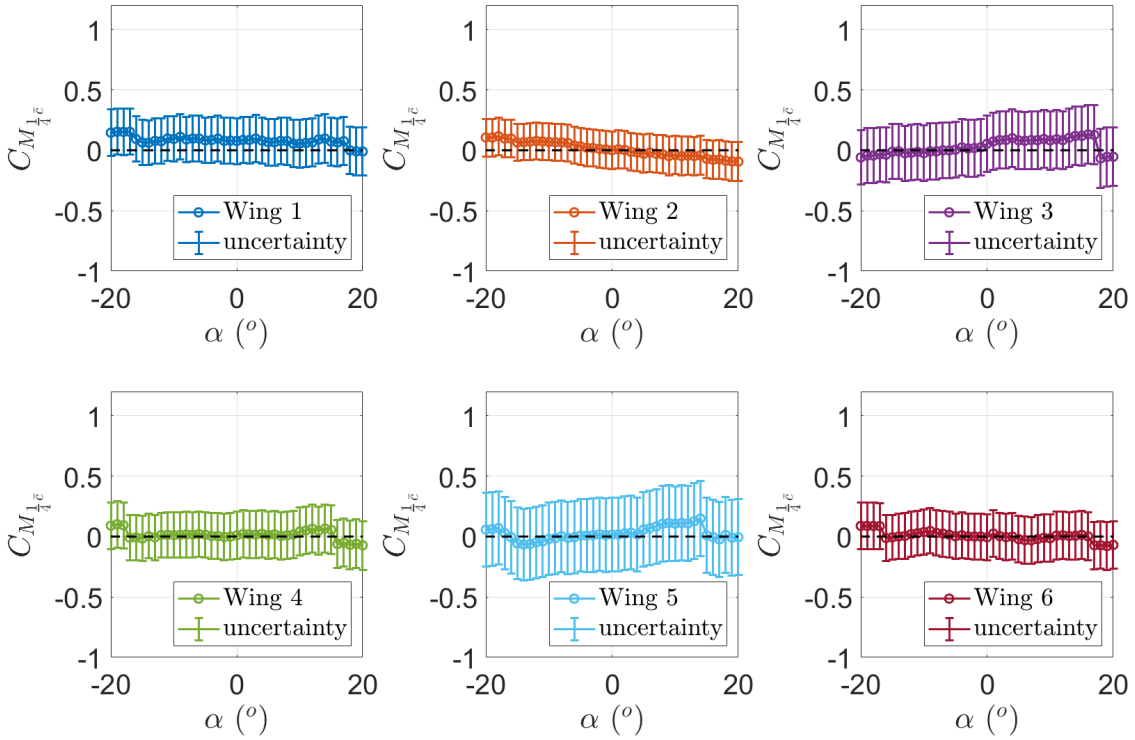

Figure 8: Coefficient of quarter-chord pitching moment vs angle of attack for all wings.

Relevant data from Figure 8 is tabulated in Table 9 including the moment about the quarter chord, the quarter chord moment coefficient, and their respective uncertainties for each wing arrangement.

Table 9: Average pitching moments and coefficients of pitching moments about the quarter-chord of each wing.

Wing	$M_{\frac{1}{4}\bar{c},avg}$ $(\mathrm{N}\cdot\mathrm{m})$	$\pm\epsilon_{M_{\frac{1}{4}\bar{c},avg}}$ $(\mathrm{N}\cdot\mathrm{m})$	$C_{M_{\frac{1}{4}\bar{c},avg}}$	$\pm\epsilon_{C_{M_{\frac{1}{4}\bar{c},avg}}}$
Wing 1	0.0887	0.0328	0.0807	0.0300
Wing 2	0.0138	0.0337	0.00896	0.02433
Wing 3	0.0258	0.0322	0.0304	0.0367
Wing 4	0.0143	0.0328	0.0130	0.0301
Wing 5	0.0172	0.0322	0.0261	0.0476
Wing 6	0.00531	0.03284	0.00458	0.03003

To visualize the small differences between the moment coefficients for the different wing geometries, the differences were tabulated in Table 10. In a similar way to the lift slope calculations, these differences were calculated between wing one and the theoretical such that comparisons for the varying aspect ratio, taper ratio and the addition of the winglet could be made in section 5.3.

Table 10: Difference between moment coefficients for wing geometries and theoretical data.

Wing #	$\overline{\Delta C}_{M_{\to 1}}$	$\epsilon_{\overline{\Delta C}_{M_{\to 1}}}$	$\overline{\Delta C}_{M_{\to theory}}$	$\epsilon_{\overline{\Delta C}_{M_{\to theory}}}$
1	0	0	0.0807	0.0300
2	-0.0718	0.0386	0.00896	0.02433
3	-0.0503	0.0474	0.0303	0.0367
4	-0.0676	0.0425	0.0131	0.0301
5	-0.0546	0.0563	0.0261	0.0476
6	-0.0761	0.0424	0.00458	0.03003

4.5 Lift to Drag Ratios

As a final point of analysis, the lift-to-drag ratio was plotted as a function of angle of attack. The lift, as determined from Section 4.2, and the drag, as determined from Section 4.3, represent the total lift and drag force experienced over the entirety of the wing. Figure 9 plots the ratio of lift force to drag force over the 41 angles of attack measured.

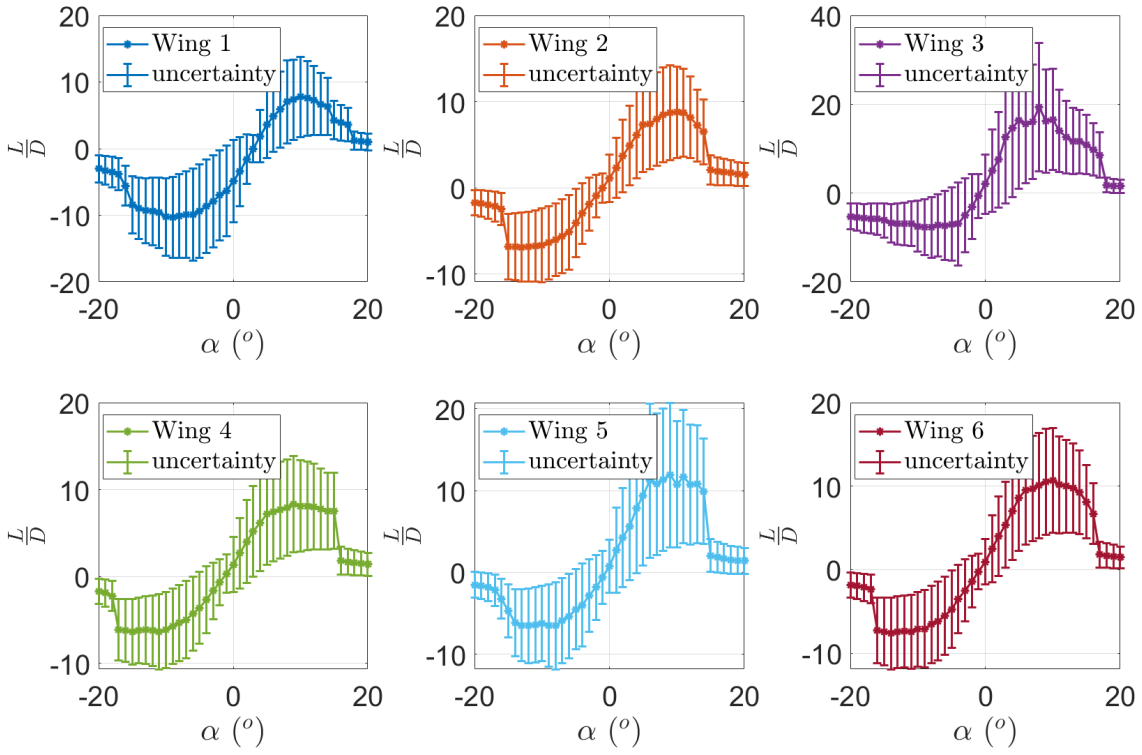

Figure 9: Lift to drag ratio vs angle of attack for all wings.

5 Discussion

5.1 Lift

The lift force as a function of angle of attack bears discussion prior to assessing the lift curve slope of the coefficient of lift. By inspection, the wings all display the characteristics of a symmetric airfoil. Figure 2 shows that the lift is zero when the angle of attack is zero, as is expected of a symmetric airfoil. Likewise, the first, third, fourth, fifth, and sixth wings each experience stall at similar magnitude angles of attack as seen from Table 5, as is also consistent with symmetric airfoils. It is important to note here that the second wing does not experience a stall angle similar in magnitude between the positive and negative angle of attack regimes. This could be due to poor data collection, which is addressed in 6.2 Recommended Improvements. Furthermore, the stall angles have a sharp drop-off in lift force values. The current experimental model has the lift force making a "shepherd's crook" shape, curving off at the stall angle at a much less aggressive angle. Additional data collection, especially around the suspected stall angle, could better show this shepherd's crook shape and better match the currently accepted lift force vs angle of attack shape.

Figure 3, which illustrates the relationship between C_L and c_L, correctly illustrates the coefficient of lift as a function of angle of attack; the greater the angle of attack, the greater

the coefficient of lift and vice versa. Additionally, the coefficient of lift increases along the airfoil. This is expected because each segment as represented in Prandtl's lifting line theory creates its own downwash that affects each segment next to it, causing more lift on the segments to the outside of it, and causing less lift on segments to the inside of it. Thus, traversing along the airfoil, the coefficient of lift increases going to the right and decreases going to the left. By this same logic, the elliptical wing in wing 5 has the same C_L as it does c_L because it is symmetric about the vertical and horizontal axes. Finally, the C_L which remains constant over the wing is by inspection proportional to the integral of c_L, which is consistent with theory.

There are several points of discussion for the coefficient of lift as a function of angle of attack, including the effect of adding winglets, how well they match theory, and general trends. As seen in Figure 4, increasing the angle of attack linearly increases the coefficient of lift. This phenomenon is true for all wings tested, but the slope of the graphs were dependent on the wing properties. This will be discussed in the following paragraphs.

Each experimental lift curve slope matches very well with the theoretical lift curve slope for that wing, as seen in Figure 4. The theoretical lift curve slopes do not account for stall angles however, so at high magnitude angles of attack, the experimental lift curve slope does not match that of the theoretical lift curve slope. From Table 6 each of the experimental lift curve slopes are greater than the theoretical lift curve slope, with the greatest discrepancy being that of the larger aspect ratio of wing 6 which is wing 1 with accompanying winglet.

Comparing the 3D lift curve slopes to the 2D lift curve slope of 2π per radian, or 0.10966 per degree, each of the theoretical and experimental lift curves are less than the idealized 2D lift curve slope. The differences between the individual wing lift slopes and the theoretical can be found in Table 7. Furthermore, the individual wings are compared to the initial testing article, wing one. An important result to consider is the difference between the high and low aspect ratio wings. In the lab testings, the data shows that the low aspect wing will have a higher lift curve slope compared to the high aspect ratio wing. This discovery should not be the case, as the aspect ratio is proportional to the lift curve slope for a finite wing. One reason that this could be observed in the results is that the force sensor crashed immediately after testing the first wing. The force sensor then required a restart, which took over 45 minutes to get running again. In starting the data collection, the second dataset may have had some startup bias which was not seen in the others. It is interesting to note that the wing with attached winglet achieves an experimental lift curve slope closest to the idealized 2D lift curve slope. This will be discussed further with other insights about the winglet addition.

The effects of the winglet addition to the wing combination of wing 6 in Figure 4 should be discussed in full. As discussed previously, the winglet combination experiences the greatest discrepancy between theoretical lift curve slope and experimental lift curve slope. Likewise, the winglet combination also experiences a lift curve slope most similar to the idealized 2D lift curve slope of 2π radians. As can be surmised from the highest lift curve slope of the wing selections, the winglet combination also obtains the highest lift force value before stalling. Thus, it can be gathered that the addition winglet increases the lift curve slope and

the lift experienced by the wing as compared to the wing combination without any winglets attached.

5.2 Drag

As seen in Figure 5 the drag is a function of the angle of attack. The point of minimum drag on each wing was located at 0°angle of attack, and the quadratic curve of the graphs show how the drag on an object grows at both positive and negative angles, which is expected for the symmetric airfoils. For each of the curves, the wings experience a stall at the angles mentioned in Table 5, where there is a jump in the amount of drag experienced by the airfoils.

Using the calculations for drag, the drag coefficients were visualized and plotted with the theoretical calculations from Prandtl's Lifting Line Theory. The coefficients of drag, as seen in Figure 6, share the same properties as their respective drag, with smaller jumps for the stall angle. For small angles, between -15 ° to 15°, the experimental curves follow the shape of the theoretical. However, in each case the theoretical curve is slightly lower than the data measured, no matter the wing geometry. This discrepancy is due to the fact that the force balance used in the lab measured the total drag, and the lifting-line theory only calculates the induced drag as a function of the angle of attack. Because the total drag contributions for a finite wing can be split between parasitic and induced drag, the difference between the experimental and theoretical plots accounts for the individual parasitic drag for each wing geometry. In this lab, wave drag was not present as there were no shocks within the wind tunnel.

The effect of the differing aspect ratios should be analyzed. Comparing the drag coefficients between wings 1–3 the measured drag coefficient does not stay the same. Although the changes are small, looking at Table 8, the smaller aspect ratio wing increases its coefficient of drag. Likewise, the contrapositive is true, as the length of the wing is increased, then the further the tips are from the symmetric plane and the lower the induced drag on the geometry for the high aspect ratio wing. In order to draw conclusions about the relative contribution of parasitic drag on the wing, the comparison to theoretical. The force balance used in the lab measured the total drag generated on the wing at different angles of attack. Meaning that the difference found in Table 8 is the theoretical parasitic drag of the wing geometry. Important to note is that this value of parasitic drag is purely based off of the theoretical induced drag from Prandtl's Lifting Line, and may be different from an experimentally tested induced drag.

A similar analysis can be made using the different wings of varying taper ratios. Comparing wings 1 and 4, by tapering the geometry of the finite wing, the overall drag of the wing decreased. Although a small difference, the tapered wing decreases the overall amount of drag by decreasing the induced drag on the wing.

Finally, the effect of the winglet addition is also a concern. Referring to the tabulated results in Table 8, the addition of the winglet increases the overall drag for the wing geometry. This increase in drag is despite the fact that the winglets themselves reduces the strength

of the wingtip vortices, and consequentially the downwash and induced drag. As such, the resultant drag is caused by the increase in parasitic drag. As the parasitic drag is broken down into both skin friction and form drag, the addition of the winglet would increase the skin friction with the extra surface area, and the form drag would go up because of the increased flow separation throughout turning.

5.3 Pitching Moment

As mentioned in 4.4 Pitching Moment, the sensor input via the sensitivity data given in Table 4 found the moment about the half-chord location of the wing. This value is not as pertinent and relevant to aerodynamic discussion and application as the moment about the quarter chord. This is because the quarter chord on an airfoil is typically considered the aerodynamic center of the airfoil, the point at which the aerodynamic moment does not change as a function of the angle of attack. This allows the aerodynamic forces relevant to aerospace applications such as lift and drag to be placed at a point where the moment is unchanging with angle of attack. To get the quarter chord moment from the half chord moment, a force moment couple system was used, and the resulting quarter chord moment coefficient was plotted.

As consistent with theory, the quarter chord moment coefficient remained about zero for each angle of attack, with values slightly deviating at the angle of attacks of greatest magnitude. This is because the aerodynamic center of an airfoil is also the center of pressure for symmetric airfoils, and the moment at the center of pressure is always constant at zero regardless of angle of attack. Comparing the standard airfoil in wing 1 with one of less aspect ratio in wing 2, there appears to be a negative slope to the quarter chord moment coefficient, just as there appears to be a positive slope to the quarter chord moment coefficient for the wing with greater aspect ratio in wing 3. This however is due to an anomaly in the data, as the quarter chord moment coefficient should still be zero for the wing regardless of how the aspect ratio may change.

Wings 4 and 5, those with taper ratio and elliptical shapes respectively, do not seem to vary from the theory already discussed; the quarter chord moment coefficient is about zero for both. The addition of the wiglet in wing 6 seems to make the quarter chord moment coefficient closest to zero out of the six different wing options. This could be due to random data anomalies, or it could be due to the reduction in induced drag and wingtip vortices affecting the wing.

5.4 Lift to Drag Ratios

As expected from both the lift and drag plots in Figure 2 and Figure 5 respectively, the lift-to-drag plot found in Figure 9 shares the symmetrical characteristics of similar magnitude stall angles in the positive and negative angle of attack regimes, similar magnitude lift to drag ratios for positive and negative angles of attack, and zero lift to drag ratio at zero degrees angle of attack.

Considering the effect of aspect ratio on the lift-to-drag ratio, it is interesting to note that wing 2, the wing variation with smaller aspect ratio, experiences the smallest lift-to-drag ratio as compared to the other wing combinations over the same range of angles of attack. By inspection, Figure 2 and Figure 5 do not illustrate a negative stall angle for wing 2, thereby increasing the lift and decreasing the drag overall as compared to other wing combinations. Additionally, wing 3 which has a higher aspect ratio experiences a much greater lift-to-drag ratio than that of the normal wing 1. Thus, it can be deduced that some sort of direct proportionality exists between the aspect ratio and lift-to-drag ratio, such that a greater aspect ratio results in a greater lift-to-drag ratio. Additionally, wing 4 which is tapered has a greater lift-to-drag ratio than wing 1, indicating that increasing the taper ratio results in higher lift-to-drag ratios as well.

It is known that the winglet addition is meant to disrupt wingtip vortices and thereby reduce the downwash and induced drag incurred by the wing. Thus, as seen from Figure 9 the lift-to-drag ratio of wing 6 is greater than that of wing 1 which features the same base wing as wing 6 but without the winglet. The addition of the winglet increases the lift and decreases the drag at the same angle of attack. One can see from the plot of lift-to-drag ratios as a function of angle that the objective of the winglet is fulfilled. The winglet decreases induced drag on the wing and thereby increases the lift-to-drag ratio as compared to the same wing without a winglet.

6 Conclusion

6.1 Summary

This lab experiment focused on the effects of changing various parameters about a symmetric airfoil, including aspect ratio, taper ratio, whether it was an elliptical wing, and the addition of a winglet. The experiment tested this by gathering pressure and voltage data for each wing from angles of attack between -20 ° and 20 ° with 1 ° increments between them. This data was then used to find lift, coefficient of lift, drag, coefficient of drag, moment about the quarter chord, and lift-to-drag ratio for each of the wings. It was determined that the winglet increased lift, lift curve slope, and lift-to-drag ratio, as well as decreasing induced drags. Increasing aspect ratio increased lift and lift-to-drag ratio, as well as decreased the induced drag on the wing. Increasing taper ratio increased lift and decreased drag. The plotting used to determine these relationships widely match the theory and thus give confidence that these relationships are valid.

6.2 Recommended Improvements

Overall, the experiment saw success in several areas. However, there are still multiple improvements that can be made:

- The best way to decrease the uncertainties in all the results and remove any noise or outlying data would be to acquire more data. The experiment provides 41 data points as the wings are rotated from $-20\,^\circ$ to $20\,^\circ$ with $1\,^\circ$ increments, but the increment

angle size could be reduced to gather more data. As seen in the previous graphs, there is not much noise that needed to be accounted for, but more data can always prove to make the results more robust and accurate.

- A major issue that the group experienced early on in the lab was the DAQ Utility not being fully connected to the sting in the test section, such that the orders to move incrementally were not received and thus not carried out. The TA present during the experiment attempted to remedy this issue after several failed attempts by resetting the entire system—both the MATLAB program and the Force/Torque transducer—only to find an issue making the two systems connect once again. After discussing with other TAs not present, the issue was eventually solved. Ensuring that the equipment that was meant to be set up prior to the experiment was connected correctly could reduce time spent idling.

Together, these improvements would make for a smoother experiment with more robust results.

References

[1] Arnold M. Kuethe, C.-Y. C., *Foundations of Aerodynamics*, John Wiley & Sons, Inc., 1998.

[2] AME 30333, *Lab 2: Circulation around a 2-D Airfoil Measured with a Five-Hole Probe*, University of Notre Dame, Notre Dame, IN, 2024.

[3] AME 30333, *Lab 4: Lift & Drag of a Finite Wing*, University of Notre Dame, Notre Dame, IN, 2024.

Appendix A - MATLAB Data Analysis Code

4/30/24 5:42 PM C:\Users\tjwel\Deskt...\dataAnalysis.m 1 of 12

```
% Lab 4 Analysis

% by Timothy Welch

clear; clc; close all

% Colors for Plots
plotColors{1} = '#0072BD'; % blue
plotColors{2} = '#D95319'; % orange
plotColors{3} = '#7E2F8E'; % purple
plotColors{4} = '#77AC30'; % green
plotColors{5} = '#4DBEEE'; % light blue
plotColors{6} = '#A2142F'; % red
plotColors{7} = '#EDB120'; % yellow
plotColors{8} = '#EBA9E5'; % pink
plotColors{9} = '#000000'; % black


doPlot = 0; % 1 = Plot; 0 = No Plot
doPlotcL = 1; % 1 = Plot; 0 = No Plot

%% Ambient Conditions
Ratm = 287; % [J/kg/K]
Tbar = 0.5*(22.2+22.3); % [*C]
Tatm = Tbar+273.15; % [K] conversion from *C
Pbar = 0.5*(980+983); % [hPa]
Patm = Pbar*100; % [Pa] conversion from hPa
ePatm = sqrt(100^2+400^2+150^2); % [Pa]
eTatm = sqrt(0.1^2+0.4^2+0.05^2); % [K]
rho = Patm/(Ratm*Tatm); % [kg/m^3]
erho = sqrt((ePatm/(Ratm*Tatm))^2+(-eTatm*Patm/(Ratm*Tatm^2))^2); % [kg/m^3]

%% Load Data and Voltage Conversion
al = -20:1:20; % [deg]
S = [50;50;50;50;39.27;50]*0.00064516; % [m^2]
c = [5;6.32;4;5;3.93;5]/39.37; % [m]
b2 = [10;7.91;12.5;10;10;10]/39.37; % [m]
wingNames = {'Wing 1','Wing 2','Wing 3','Wing 4','Wing 5','Wing 6'};
load('calConst.mat')

offsetFiles = {'offset_wing_1Cleaned.mat','offset_wing_2Cleaned.↙
mat','offset_wing_3Cleaned.mat','offset_wing_4.mat','offset_wing_5.mat','offset_wing_6.↙
mat'};
dataFiles = {'wing_1Cleaned.mat','wing_2Cleaned.mat','wing_3Cleaned.mat','wing_4.↙
mat','wing_5.mat','wing_6.mat'};
sensitivities = [0.02;0.02;0.025]; % [V/N] or [V/(Nm)]
specUncerts = [2;3;0.2]; % [N] or [Nm]

wingData = zeros(length(dataFiles),length(al),length(sensitivities)); % (wing#,alpha,↙
dataType)
```

```
eWingData = zeros(length(dataFiles),length(al),length(sensitivities)); % (wing#,alpha,↙
dataType)
for i=1:length(dataFiles)
    wing = load(dataFiles{i});
    offset = load(offsetFiles{i});
    wingData(i,:,1) = (wing.mean_data(:,1)-offset.mean_data(1))*calConst; % [Pa]
    for j=2:4
        wingData(i,:,j) = (wing.mean_data(:,j)-offset.mean_data(j))/sensitivities(j-1);
        eWingData(i,:,j) = specUncerts(j-1)*ones(1,length(al),1);
    end
end

dp = squeeze(wingData(:,:,1));
edp = squeeze(eWingData(:,:,1));

L = squeeze(wingData(:,:,2));
eL = squeeze(eWingData(:,:,2));

D = squeeze(wingData(:,:,3));
eD = squeeze(eWingData(:,:,3));

Mc2 = squeeze(wingData(:,:,4));
eMc2 = squeeze(eWingData(:,:,4));
M = zeros(length(dataFiles),length(al));
Mavg = zeros(length(dataFiles),1);
eM = zeros(length(dataFiles),length(al));
eMavg = zeros(length(dataFiles),1);
for i=1:length(dataFiles)
    M(i,:) = Mc2(i,:) - (c(i)/4)*(L(i,:).*cosd(al) + D(i,:).*sind(al));
    Mavg(i) = mean(M(i,:));
    eM(i,:) = sqrt(eMc2(i,:).^2 + (0.25*eL(i,:).*c(i).*cosd(al)).^2 + (0.25*eD(i,:).*c↙
(i).*sind(al)).^2);
    eMavg(i) = sqrt(sum(eM(i,:).^2))/length(al);
end

%% Theoretical Predictions
AR = [4;2.5;6.25;4;5.09;4];
lambda = [1;1;1;3/7;0;1]; % Taper Ratio (ct/cs)
twist = 0; % [deg]
alL0 = 0; % [deg]
k = 100;

CLTheo = zeros(length(AR),length(al));
cLTheo = zeros(length(AR),length(al),k);
CDiTheo = zeros(length(AR),length(al));
for iAR=1:length(AR)
    for iAl=1:length(al)
        [CLTheo(iAR,iAl),cLTheo(iAR,iAl,:),CDiTheo(iAR,iAl)] = liftLine(AR(iAR),lambda↙
(iAR),twist,al(iAl),alL0,k);
    end
```

```
end
cLTheo(5,:,:) = ((2*pi/(1+2*pi/(pi*AR(5))))*(pi/180)*al)' * ones(1,k);
CLTheo(5,:) = (2*pi/(1+2*pi/(pi*AR(5))))*(pi/180)*al;
CMTheo = zeros(length(AR),length(al));

%% Plot Lifts, Drags, and Moments
if doPlot
    % Plot Lift
    figure
    for i=1:length(dataFiles)
        subplot(2,3,i)
        plot(al,L(i,:),'s-','Color',plotColors{i},'Linewidth',1.5)
        hold on
    end
    for i=1:length(dataFiles)
        subplot(2,3,i)
        errorbar(al,L(i,:),eL(i,:),'vertical','Color',plotColors{i},'Linewidth',1.5)
        set(gca,'fontSize',20)
        grid on
        xlabel('$\alpha$ ($^o$)','interpreter','latex')
        ylabel('$L$ (N)','interpreter','latex')
        legend(wingNames{i},'uncertainty','Location','southeast','interpreter','latex')
    end
    hold off

    % Plot Drag
    figure
    for i=1:length(dataFiles)
        subplot(2,3,i)
        plot(al,D(i,:),'^-','Color',plotColors{i},'Linewidth',1.5)
        hold on
    end
    for i=1:length(dataFiles)
        subplot(2,3,i)
        errorbar(al,D(i,:),eD(i,:),'vertical','Color',plotColors{i},'Linewidth',1.5)
        set(gca,'fontSize',20)
        grid on
        xlabel('$\alpha$ ($^o$)','interpreter','latex')
        ylabel('$D$ (N)','interpreter','latex')
        legend(wingNames{i},'uncertainty','Location','north','interpreter','latex')
        ylim([-3,8])
    end
    hold off

    % Plot Moment
    figure
    for i=1:length(dataFiles)
        subplot(2,3,i)
        plot(al,M(i,:),'o-','Color',plotColors{i},'Linewidth',1.5)
        hold on
```

```
    end
    for i=1:length(dataFiles)
        subplot(2,3,i)
        errorbar(al,M(i,:),eM(i,:),'vertical','Color',plotColors{i},'Linewidth',1.5)
        set(gca,'fontSize',20)
        grid on
        xlabel('$\alpha$ ($^o$)','interpreter','latex')
        ylabel('$M_{\frac{1}{4}\bar{c}}$ (N$\cdot$m)','interpreter','latex')
        legend(wingNames{i},'uncertainty','Location','southeast','interpreter','latex')
        ylim([-1,1])
    end
    hold off
end

%% Calculate CL, CD, and CM
CL = zeros(length(S),length(L(1,:)));
CD = zeros(length(S),length(D(1,:)));
CM = zeros(length(S),length(M(1,:)));
eCL = zeros(length(S),length(L(1,:)));
eCD = zeros(length(S),length(D(1,:)));
eCM = zeros(length(S),length(M(1,:)));
CMavg = zeros(length(dataFiles),1);
eCMavg = zeros(length(dataFiles),1);
m = zeros(length(S),1);
mTheo = zeros(length(S),1);
m0 = zeros(length(S),1);
em = zeros(length(S),1);
for i=1:length(S)
    CL(i,:) = L(i,:)./(dp(i,:)*S(i));
    CD(i,:) = D(i,:)./(dp(i,:)*S(i));
    CM(i,:) = M(i,:)./(dp(i,:)*S(i)*c(i));

    CMavg(i,:) = mean(CM(i,:));

    pm = polyfit(al(9:33),CL(i,9:33),1);
    m(i) = pm(1);
    pmTheo = polyfit(al(9:33),CLTheo(i,9:33),1);
    mTheo(i) = pmTheo(1);
    m0(i) = pi^2/90;

    eCL(i,:) = eL(i,:)./(dp(i,:)*S(i));
    eCD(i,:) = eD(i,:)./(dp(i,:)*S(i));
    eCM(i,:) = eM(i,:)./(dp(i,:)*S(i)*c(i));

    eCMavg(i,:) = sqrt(sum(eCM(i,:).^2))/length(al);

    eCLDiffTotal = 0;
    for j=1:(33-9)
        eCLDiff = (eCL(i,j+1)-eCL(i,j))^2;
        eCLDiffTotal = eCLDiffTotal+eCLDiff;
```

```
    end
    em(i) = sqrt(eCLDiffTotal/24);
end

% Create Table for lift curve slopes
m0T = num2cell(m0);
mTheoT = num2cell(mTheo);
mT = num2cell(m);
emT = num2cell(em);
T1 = array2table([wingNames',m0T,mTheoT,mT,emT],'VariableNames',{'Wing','m_0','m_↙
{theo}','m','\epsilon_m',});
table2latex(T1,'mTab')

% Create Table for average moments
MavgT = num2cell(Mavg);
eMavgT = num2cell(eMavg);
CMavgT = num2cell(CMavg);
eCMavgT = num2cell(eCMavg);
T2 = array2table([wingNames',MavgT,eMavgT,CMavgT,eCMavgT],...
    'VariableNames',{'Wing','$M_{\frac{1}{4}\bar{c},avg}$',...
    '$\epsilon_{M_{\frac{1}{4}\bar{c},avg}}$',...
    '$C_{M_{\frac{1}{4}\bar{c},avg}}$',...
    '$\epsilon_{C_{M_{\frac{1}{4}\bar{c},avg}}}$',});
table2latex(T2,'Mavg')

%% Plot CL, CD, and CM
if doPlot
    % Plot Lift Coefficient
    figure
    for i=1:length(dataFiles)
        subplot(2,3,i)
        plot(al,CL(i,:),'s-','Color',plotColors{i},'Linewidth',1.5)
        hold on
    end
    for i=1:length(dataFiles)
        subplot(2,3,i)
        errorbar(al,CL(i,:),eCL(i,:),'vertical','Color',plotColors{i},'Linewidth',1.5)
        plot(al,CLTheo(i,:),'k--','Linewidth',1.5)
        set(gca,'fontSize',20)
        grid on
        xlabel('$\alpha$ ($^o$)','interpreter','latex')
        ylabel('$C_L$','interpreter','latex')
        legend(wingNames↙
{i},'uncertainty','theoretical','Location','southeast','interpreter','latex')
    end
    hold off

    % Plot Drag Coefficient
    figure
    for i=1:length(dataFiles)
```

```
        subplot(2,3,i)
        plot(al,CD(i,:),'^-','Color',plotColors{i},'Linewidth',1.5)
        hold on
    end
    for i=1:length(dataFiles)
        subplot(2,3,i)
        errorbar(al,CD(i,:),eCD(i,:),'vertical','Color',plotColors{i},'Linewidth',1.5)
        plot(al,CDiTheo(i,:),'k--','Linewidth',1.5)
        set(gca,'fontSize',20)
        grid on
        xlabel('$\alpha$ ($^o$)','interpreter','latex')
        ylabel('$C_D$','interpreter','latex')
        legend(wingNames↙
{i},'uncertainty','theoretical','Location','north','interpreter','latex')
        ylim([-0.5,1.5])
    end
    hold off

    % Plot Moment Coefficient
    figure
    for i=1:length(dataFiles)
        subplot(2,3,i)
        plot(al,CM(i,:),'o-','Color',plotColors{i},'Linewidth',1.5)
        hold on
    end
    for i=1:length(dataFiles)
        subplot(2,3,i)
        errorbar(al,CM(i,:),eCM(i,:),'vertical','Color',plotColors{i},'Linewidth',1.5)
        plot(al,CMTheo(i,:),'k--','Linewidth',1.5)
        set(gca,'fontSize',20)
        grid on
        xlabel('$\alpha$ ($^o$)','interpreter','latex')
        ylabel('$C_{M_{\frac{1}{4}\bar{c}}}$','interpreter','latex')
        legend(wingNames{i},'uncertainty','Location','southeast','interpreter','latex')
        ylim([-1,1.2])
    end
    hold off

    % Plot Moment Coefficient vs Lift Coefficient
    figure
    for i=1:length(dataFiles)
        subplot(2,3,i)
        plot(CL(i,:),CM(i,:),'o-','Color',plotColors{i},'Linewidth',1.5)
        hold on
    end
    for i=1:length(dataFiles)
        subplot(2,3,i)
        errorbar(CL(i,:),CM(i,:),eCM(i,:),'vertical','Color',plotColors{i},'Linewidth',↙
1.5)
        errorbar(CL(i,:),CM(i,:),eCL(i,:),'horizontal','Color',plotColors↙
```

```
{i},'Linewidth',1.5)
        set(gca,'fontSize',20)
        grid on
        xlabel('$\alpha$ ($^o$)','interpreter','latex')
        ylabel('$C_{M_{\frac{1}{4}\bar{c}}}$','interpreter','latex')
        legend(wingNames{i},'uncertainty','Location','southeast','interpreter','latex')
    end
    hold off
end

%% Plot cLTheo
% New Colors for Plots
plotColorsDark{1} = '#015287'; % dark blue
plotColorsDark{2} = '#A13E13'; % dark orange
plotColorsDark{3} = '#4D1D57'; % dark purple
plotColorsDark{4} = '#4F7320'; % darkgreen
plotColorsDark{5} = '#337E9E'; % dark light blue

legendLabels1 = ["$\alpha$ = "+num2str(al(31))+"$^o$",'',...
                 "$\alpha$ = "+num2str(al(26))+"$^o$",'',...
                 "$\alpha$ = "+num2str(al(21))+"$^o$",'',...
                 "$\alpha$ = "+num2str(al(16))+"$^o$",'',...
                 "$\alpha$ = "+num2str(al(11))+"$^o$",''];
legendLabels2 = ["$C_L$","$c_L$"];

if doPlotcL
    figure
    for i=1:length(dataFiles)
        subplot(2,3,i)
        for j=length(al)-10:-5:11
            plot(linspace(0,b2(i),k),CLTheo(i,j)*ones(1,k),'-','Color',plotColors{(j-↙
36)/-5},'Linewidth',1.5)
            hold on
            plot(linspace(0,b2(i),k),squeeze(cLTheo(i,j,:)),'--','Color',plotColorsDark↙
{(j-36)/-5},'Linewidth',1.5)
            set(gca,'fontSize',20)
            grid on
            xlabel('y (m)','interpreter','latex')
            ylabel('$C_L$ \& $c_L$','interpreter','latex')
        end
        xlim([0,b2(i)])
        hold off
        switch i
            case 1
                legend(legendLabels1,'Location','none','interpreter','latex')
            case 2
                legend(legendLabels2,'Location','none','interpreter','latex')
        end
    end
end
```

```
%% Calculate Lift to Drag Ratio
LDRat = L./D;
eLDRat = sqrt(abs(eL./D) + abs(eD.*L./D.^2));

%% Plot Lift and Drag Ratio
if doPlot
    figure
    for i=1:length(dataFiles)
        subplot(2,3,i)
        plot(al,LDRat(i,:),'*-','Color',plotColors{i},'Linewidth',1.5)
        hold on
    end
    for i=1:length(dataFiles)
        subplot(2,3,i)
        errorbar(al,LDRat(i,:),eLDRat(i,:),'vertical','Color',plotColors↙
{i},'Linewidth',1.5)
        set(gca,'fontSize',20)
        grid on
        xlabel('$\alpha$ ($^o$)','interpreter','latex')
        ylabel('$\frac{L}{D}$','interpreter','latex')
        legend(wingNames{i},'uncertainty','Location','best','interpreter','latex')
    end
    hold off
end

%% Comparison to Wing 1 and Theory
dm1 = zeros(length(dataFiles),1);
dCD1 = zeros(length(dataFiles),length(al));
dCM1 = zeros(length(dataFiles),length(al));
dmth = zeros(length(dataFiles),1);
dCDth = zeros(length(dataFiles),length(al));
dCMth = zeros(length(dataFiles),length(al));

edm1 = zeros(length(dataFiles),1);
edCD1 = zeros(length(dataFiles),length(al));
edCM1 = zeros(length(dataFiles),length(al));
edmth = zeros(length(dataFiles),1);
edCDth = zeros(length(dataFiles),length(al));
edCMth = zeros(length(dataFiles),length(al));

dCD1avg = zeros(length(dataFiles),1);
dCM1avg = zeros(length(dataFiles),1);
dCDthavg = zeros(length(dataFiles),1);
dCMthavg = zeros(length(dataFiles),1);

edCD1avg = zeros(length(dataFiles),1);
edCM1avg = zeros(length(dataFiles),1);
edCDthavg = zeros(length(dataFiles),1);
edCMthavg = zeros(length(dataFiles),1);
```

```
for i=1:length(dataFiles)
    dm1(i) = m(i)-m(1);
    dCD1(i,:) = CD(i,:)-CD(1,:);
    dCM1(i,:) = CM(i,:)-CM(1,:);

    edm1(i) = sqrt((em(i)).^2 + (em(1)).^2);
    edCD1(i,:) = sqrt((eCD(i,:)).^2 + (eCD(1,:)).^2);
    edCM1(i,:) = sqrt((eCM(i,:)).^2 + (eCM(1,:)).^2);

    dmth(i) = m(i)-m0(i);
    dCDth(i,:) = CD(i,:)-CDiTheo(i,:);
    dCMth(i,:) = CM(i,:)-CMTheo(i,:);

    edmth(i) = em(i);
    edCDth(i,:) = eCD(i,:);
    edCMth(i,:) = eCM(i,:);

    dCD1avg(i) = mean(dCD1(i,:));
    dCM1avg(i) = mean(dCM1(i,:));

    edCD1avg(i) = sqrt(sum(edCD1(i,:).^2))/length(al);
    edCM1avg(i) = sqrt(sum(edCM1(i,:).^2))/length(al);

    dCDthavg(i) = mean(dCDth(i,:));
    dCMthavg(i) = mean(dCMth(i,:));

    edCDthavg(i) = sqrt(sum(edCDth(i,:).^2))/length(al);
    edCMthavg(i) = sqrt(sum(edCMth(i,:).^2))/length(al);
end

% Make into Tables
dm1T = num2cell(dm1);
edm1T = num2cell(edm1);
dmthT = num2cell(dmth);
edmthT = num2cell(edmth);
T3 = array2table([wingNames',dm1T,edm1T,dmthT,edmthT],...
    'VariableNames',{'Wing','1',...
    '2',...
    '3',...
    '4',});
table2latex(T3,'liftDiffs')

dCD1T = num2cell(dCD1avg);
edCD1T = num2cell(edCD1avg);
dCDthT = num2cell(dCDthavg);
edCDthT = num2cell(edCDthavg);
T4 = array2table([wingNames',dCD1T,edCD1T,dCDthT,edCDthT],...
    'VariableNames',{'Wing','1',...
    '2',...
```

```
    '3',...
    '4',});
table2latex(T4,'dragDiffs')

dCM1T = num2cell(dCM1avg);
edCM1T = num2cell(edCM1avg);
dCMthT = num2cell(dCMthavg);
edCMthT = num2cell(edCMthavg);
T5 = array2table([wingNames',dCM1T,edCM1T,dCMthT,edCMthT],...
    'VariableNames',{'Wing','1',...
    '2',...
    '3',...
    '4',});
table2latex(T5,'momDiffs')

%% Functions
function [varargout] = liftLine(AR,lambda,twist,al,alL0,k)
    % Convert to Radians
    twist = twist*pi/180; al = al*pi/180; alL0 = alL0*pi/180;

    % Calculate Important Parameters
    th = zeros(k,1); Y = zeros(k,1); C = zeros(k,1); D = zeros(k,k); ala = zeros(k,1);

    for j = 1:k
        th(j) = (pi/2)*(j/k);
        Y(j) = cos(th(j));
        C(j) = 1-(1-lambda)*cos(th(j));
        for n = 1:k
            D(j,n) = (1/C(j) + (2*n-1)*pi/(AR*(1+lambda)*sin(th(j))))*sin((2*n-1)*th
(j));
        end
        ala(j) = (al - alL0) + twist*cos(th(j)); % Absolute AoA [rad]
    end

    % Solve the System D*An=ala for An
    A = D\ala;

    % Calculate Performance Parameters
    CL = A(1)*pi^2/(1+lambda);

    cL = zeros(k,1);
    for j=1:k
        sum1 = 0;
        for n=1:k
            sum1 = sum1 + A(n)*sin((2*n-1)*th(j));
        end
        cL(j) = 2*pi*sum1/C(j);
    end

    sum2 = 0;
```

```
    for n=1:k
        sum2 = sum2 + (2*n-1)*A(n)^2;
    end

    CDi = pi^3/(AR*(1+lambda)^2)*sum2;

    varargout = {CL;cL;CDi};
end

function table2latex(T, filename)

    % Error detection and default parameters
    if nargin < 2
        filename = 'table.tex';
        fprintf('Output path is not defined. The table will be written in %s.\n',↙
filename);
    elseif ~ischar(filename)
        error('The output file name must be a string.');
    else
        if ~strcmp(filename(end-3:end), '.tex')
            filename = [filename '.tex'];
        end
    end
    if nargin < 1, error('Not enough parameters.'); end
    if ~istable(T), error('Input must be a table.'); end

    % Parameters
    n_col = size(T,2);
    col_spec = [];
    for c = 1:n_col, col_spec = [col_spec 'l']; end
    col_names = strjoin(T.Properties.VariableNames, ' & ');
    row_names = T.Properties.RowNames;
    if ~isempty(row_names)
        col_spec = ['l' col_spec];
        col_names = ['& ' col_names];
    end

    % Writing header
    fileID = fopen(filename, 'w');
    fprintf(fileID, '\\begin{tabular}{%s}\n', col_spec);
    fprintf(fileID, '%s \\\\ \n', col_names);
    fprintf(fileID, '\\hline \n');

    % Writing the data
    try
        for row = 1:size(T,1)
            temp{1,n_col} = [];
            for col = 1:n_col
                value = T{row,col};
                if isstruct(value), error('Table must not contain structs.'); end
```

```
                while iscell(value), value = value{1,1}; end
                if isinf(value), value = '$\infty$'; end
                temp{1,col} = num2str(value);
            end
            if ~isempty(row_names)
                temp = [row_names{row}, temp];
            end
            fprintf(fileID, '%s \\\\ \n', strjoin(temp, ' & '));
            clear temp;
        end
    catch
        error('Unknown error. Make sure that table only contains chars, strings or↙
numeric values.');
    end

    % Closing the file
    fprintf(fileID, '\\hline \n');
    fprintf(fileID, '\\end{tabular}');
    fclose(fileID);
end
```